Survey of Solution Techniques for Linear Systems from Finite Difference Methods in 2D Numerical Radiative Transfer

Advanced Numerical Analysis II Final Project

Oliver Evans
Fred Weiss
Christopher Parker
Emmanuel Arkoh

Dr. Malena Español

May 12, 2017

1 Introduction

We use monochromatic radiative transfer in order to model the light field in an aqueous environment populated by vegetation. The vegetation (kelp) is modeled by a spatial probability distribution, which we assume to be given. The two quantities we seek to compute are *radiance* and *irradiance*. Radiance is the intensity of light in at a particular point in a particular direction, while irradiance is the total light intensity at a point in space, integrated over all angles. The Radiative Transfer Equation is an integro-partial differential equation for radiance, which has been used primarily in stellar astrophysics; it's application to marine biology is fairly recent [9].

We study various methods for solving the system of linear equations resulting from discretizing the Radiative Transfer Equation. In particular, we consider direct methods, stationary iterative methods, and nonstationary iterative methods. Numerical experiments are performed using Python's `scipy.sparse` [8] package for sparse linear algebra. `IPython` [11] was used for interactive numerical experimentation.

Among those implemented, the nonstationary LGMRES [4] algorithm is the only algorithm determined to be suitable for this application without further work. We discuss limitations and potential improvements, including preconditioning, alternative discretization, and reformulation of the RTE.

1.1 Radiative Transfer

Let n be the number of spatial dimensions for the problem (i.e., 2 or 3). Let $x \in \mathcal{R}^n$. Let Ω be the unit sphere in $\mathcal{R}^n$. Let $\omega \in \Omega$ be a unit vector in $\mathcal{R}^n$. Let $L(x, \omega)$ denote *radiance* position x in the direction ω. Let $I(x)$ denote *irradiance* at position x. Let $P_k(x)$ be the probability density of kelp at position x. Let $a(x)$ and $b(x)$ denote the absorption and scattering coefficients respectively of the medium, which are both functions of P_k. Let $\beta(\Delta\theta)$ denote the normalized *volume scattering function* or *phase function*, which defines the probability of light scattering at an angle $\Delta\theta$ from it's initial direction in a scattering event.

Then, the Monochromatic Time-Independent Radiative Transfer Equation (RTE) is

$$\omega \cdot \nabla_x L(x,\omega) = -(a(x)+b(x))L(x,\omega) + b\int_\Omega \beta(\omega\cdot\omega')L(x,\omega')\,d\omega' \qquad \text{(RTE)}$$

Note that in 2 spatial dimensions, this is a 3-dimensional problem (x, y, θ). Likewise, in 3 spatial dimensions, it is a 5-dimensional problem (x, y, z, θ, ϕ).

In this paper, we consider only the 2-dimensional problem, with the hope that sufficiently robust solution techniques for the 2-dimensional problem will be effective in the solution of the 3-dimensional problem, as well.

1.2 2D Problem

We use the downward-pointing coordinate system shown in figure 1, measuring $\theta \in [0, 2\pi)$ from the positive x axis towards the positive y axis. Further, we assume that the problem is given on the rescaled spatial domain $[0, 1)\times[0, 1)$, where $y = 0$ is the air-water interface, and y measures depth from the surface.

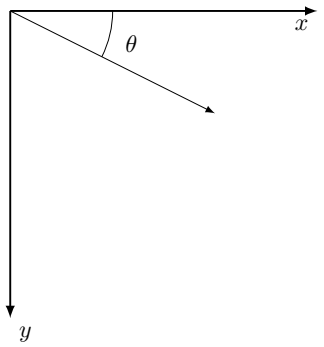

Figure 1: 2D coordinate system

The 2-dimensional form of (RTE) is given by

$$\frac{\partial L}{\partial x}\cos\theta + \frac{\partial L}{\partial y}\sin\theta = -(a+b)L(x,y,\theta) + b\int_0^{2\pi}\beta(|\theta-\theta'|)\,d\theta', \qquad (1)$$

where $|\theta - \theta'|$ measures the smallest angular difference between $]thet$ and θ' considering periodicity.

Note that in Cartesian coordinates, there are only spatial, not angular derivatives in the gradient. In other coordinate systems, this is generally not the case.

1.3 Boundary Conditions

We assume that the downwelling light from the surface is known, and is defined to be uniform in space by the Dirichlet boundary condition

$$L(x, 0, \theta) = f(\theta), \quad \text{for} \quad \theta \in [0, \pi). \qquad (2)$$

Note that we cannot apply the same idea to upwelling light at the surface, as it cannot be specified from information about the atmospheric light field. Therefore, we apply the PDE at $y = 0$ for $\theta \in [\pi, 2\pi)$.

At $y = 1$, we assume no upwelling light. That is,

$$L(x, 0, \theta) = 0, \quad \text{for} \quad \theta \in [\pi, 2\pi). \qquad (3)$$

As with the upper y-boundary, we apply the PDE for $\theta \in [0, \pi)$ so as not to prohibit downwelling light.

In the horizontal direction, we assume periodic boundary conditions. Assuming that a single discrete group of plants is being simulated, adjusting the width of the domain effectively modifies the spacing between adjacent groups of plants.

2 System of Linear Equations

2.1 Discretization

In order to solve (1) numerically, we discretize the spatial derivatives using 2nd order finite difference approximations, and we discretize the integral according to the Legendre-Gauss quadrature, as described in Chandrasekhar [5, Chapter 2]. With this in mind, in order to create a spatial-angular grid with n_x, n_y, and n_θ discrete values for x, y, and θ respectively, we use a uniform square spatial discretization with spacing dx, dy, and a non-uniform angular discretization according to the roots of the Legendre Polynomial of degree n_θ, denoted $P_{n_\theta}(\theta)$. In each variable, we discard the uppermost grid point, as indicated by the half-open intervals in the previous sections.

Then, we have the grid

$$x_i = (i-1)\,dx, \qquad i = 1, \ldots, n_x \tag{4}$$
$$y_j = (j-1)\,dy, \qquad j = 1, \ldots, n_y \tag{5}$$
$$\theta_k \text{ s.t. } P_{n_\theta}(\theta_k/\pi - 1) = 0, \qquad k = 1, \ldots, n_\theta \tag{6}$$

In the same notational vein, let

$$L^k_{ij} = L(x_i, y_j, \theta_k), \tag{7}$$
$$\beta_{kl} = \beta(|\theta_k - \theta_l|), \tag{8}$$
$$a_{ij} = a(x, y) \tag{9}$$
$$b_{ij} = b(x, y) \tag{10}$$

where $|\cdot|$ is periodic as in (1).

For the spatial interior of the domain, we use the 2nd order central difference formula (CD2) to approximate the derivatives, which is

$$f'(x) = \frac{f(x+dx) - f(x-dx)}{2dx} + \mathcal{O}(dx^3). \tag{CD2}$$

When applying the PDE on the upper or lower boundary, we use the forward and backward difference (FD2 and BD2) formulas respectively. Omitting $\mathcal{O}(dx^3)$, we have

$$f'(x) = \frac{-3f(x) + 2f(x+dx) - f(x+2dx)}{2dx} \tag{FD2}$$

$$f'(x) = \frac{3f(x) - 2f(x-dx) + f(x-2dx)}{2dx} \tag{BD2}$$

As for the angular integral, we substitute a weighted finite sum of the function evaluated at the angular grid points. For each k, let a_k be the appropriate Legendre-Gauss weight according to Chandrasekhar [5, Chapter 2]. Then, applying the change of variables theorem to transform from the standard quadrature interval $[0, 1]$ to the correct angular interval $[0, 2\pi]$, we have

$$\int_0^{2\pi} f(\theta)\,d\theta \approx \pi \sum_{k=1}^{n} a_k f(\theta_k) \tag{LG}$$

2.2 Difference Equation

Given the above discrete approximations, the difference equation for (RTE) in the spatial interior of the domain is

$$\begin{aligned} 0 = {} & \frac{1}{2dx}\left(L^k_{i+1,j} - L^k_{i-1,j}\right)\cos\theta_k - \pi b \sum_{\substack{l=1 \\ l\neq k}}^{n_\theta} a_l \beta_{kl} L^l_{ij} \\ & + \frac{1}{2dy}\left(L^k_{i,j+1} - L^k_{i,j+1}\right)\sin\theta_k + (a_{ij} + b_{ij}) L^k_{ij} \end{aligned} \tag{11}$$

Similarly, we discretize using (FD2) and (BD2) at the boundaries. For example, when $j = 1$, we have

$$\begin{aligned} 0 = {} & \frac{1}{2dx}\left(L^k_{i+1,j} - L^k_{i-1,j}\right)\cos\theta_k - \pi b \sum_{\substack{l=1 \\ l\neq k}}^{n_\theta} a_l \beta_{kl} L^l_{ij} \\ & + \frac{1}{2dy}\left(4L^k_{i,j+1} - L^k_{i,j+2}\right)\sin\theta_k + (a_{ij} + b_{ij} - \frac{3}{2dy}) L^k_{ij} \end{aligned} \tag{12}$$

Note that when discretizing the integral, we exclude the $l = k$ term of the sum. This is because that term corresponds to "scattering" straight ahead ($\Delta\theta = 0$), which is in fact not scattering at all. Whether some adjustment to the quadrature is necessary to account for this is unclear.

2.3 Structure of Linear System

For each (i, j, k), we have a distinct equation with $4 + n_\theta$ variables. This corresponds to a sparse matrix equation $Ax = b$, each row having $4 + n_\theta$ nonzero entries. Note that b is zero at each row except those which correspond to boundary conditions in y.

Each element in x and b correspond to a particular triple (i, j, k), as are each row and column of the coefficient matrix A. In some sense, when we create this linear system, we are unwrapping a 3-dimensional quantity (radiance) into a 1-dimensional vector (the solution, x). Different orders in which the equations are listed can be chosen to generate equivalent systems, so long as the ordering is consistent in A, b, and x.

The most obvious way to order the equations is to do so via a triple `for` loop, which has the effect of creating blocks in the matrix corresponding to planes in (x, y, θ) space. For example, if the equations are ordered such that the outer `for` loop is over x, and the inner two are over y and θ, then the first $(n_y n_\theta)$ rows of the matrix correspond to the equations for $i = 1$.

By switching the order of the `for` loops, we can generate 6 equivalent matrix systems, each of which can be identified with a permutation of the triple $(0, 1, 2)$, where 0 corresponds to x, 1 corresponds to y, and 2 corresponds to θ, and the order of the numbers indicates the order in which the loops were nested, from outer to inner.

The coefficient matrices A, generated by each of these choices are shown below for a trivially small system with $n_x = n_y = n_\theta = 6$. Each black square represents a nonzero entry, whereas gray lines are purely for visual aid.

2.4 Sparsity Plots

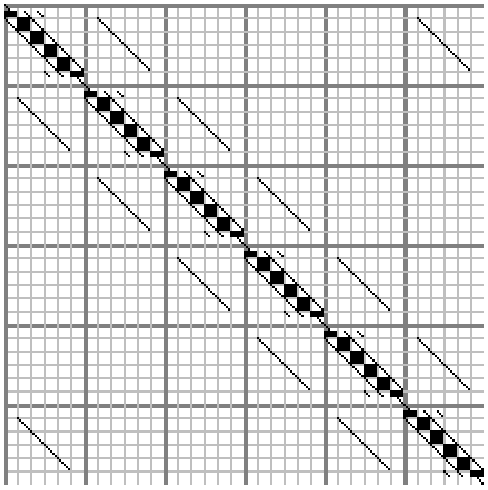

Figure 2: Sparsity plot: 6x6x6, ordering 012

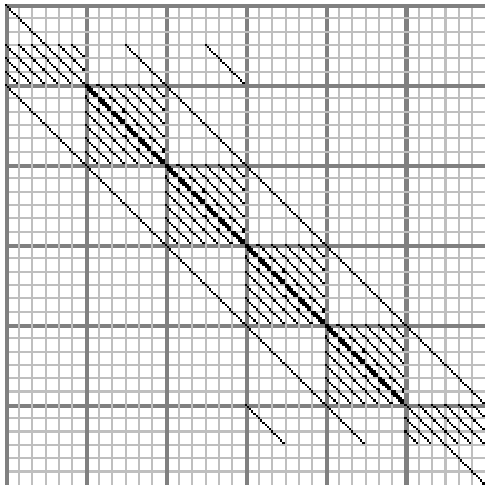

Figure 5: Sparsity plot: 6x6x6, ordering 120

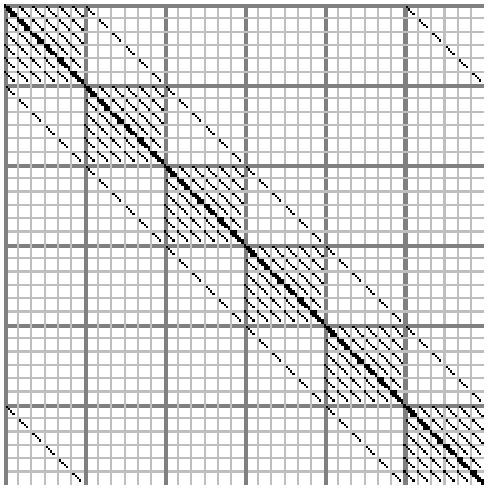

Figure 3: Sparsity plot: 6x6x6, ordering 021

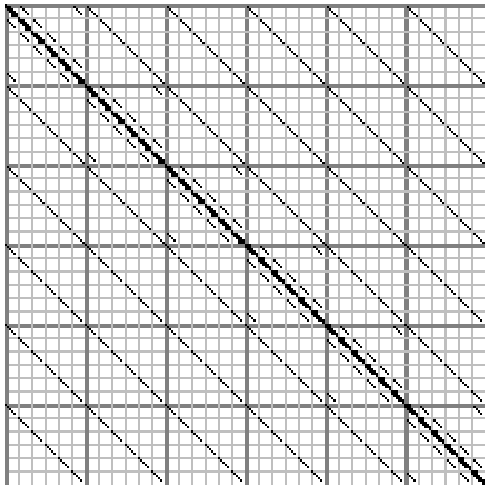

Figure 6: Sparsity plot: 6x6x6, ordering 201

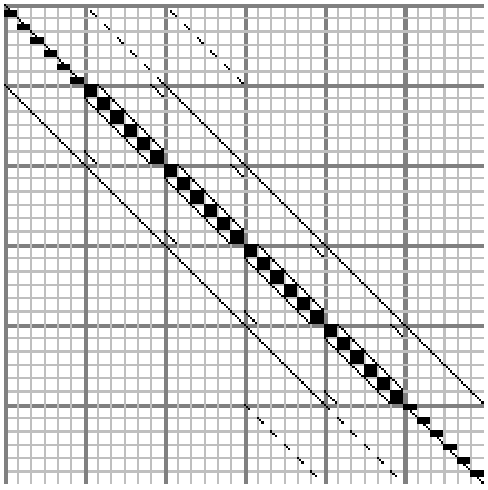

Figure 4: Sparsity plot: 6x6x6, ordering 102

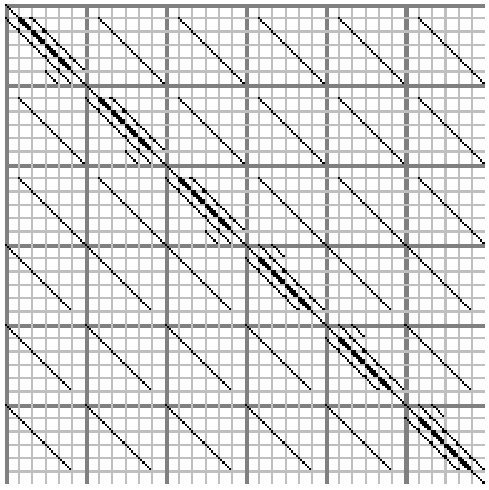

Figure 7: Sparsity plot: 6x6x6, ordering 210

2.5 Matrix Properties

There are several properties which a real matrix can have which simplify or accelerate the solution procedure. The first is symmetry. Simply from the sparsity patters, we see that none of the above matrices are symmetric. A symmetric matrix can additionally be positive definite, in which case numerous highly efficient algorithms exist for solving the system, such as the Conjugate Gradient method [10]. Another important property is diagonal dominance.

2.5.1 Diagonal Dominance

A matrix $A = (a_ij)$ is said to be diagonally dominant if

$$|a_{jj}| > \sum_{i \neq j} |a_{ij}| \text{ for all } i \tag{13}$$

For each i, define the quantities

$$\mathcal{D}_i = |a_{jj}| \tag{14}$$

$$\mathcal{N}_i = \sum_{i \neq j} |a_{ij}| \tag{15}$$

$$\mathcal{D}_i = \mathcal{D}_i - \mathcal{N}_i \tag{16}$$

Then, A is diagonally dominant if and only if

$$\min_{1 \leq i \leq n} \mathcal{D}_i > 0 \tag{17}$$

3 Direct Methods

3.1 Factorizations

The most straightforward way to solve any linear system is via Gaussian Elimination, or equivalently, by performing an LU factorization. However, the number of arithmetic operations required for full LU factorization algorithm grows as $\mathcal{O}(n^3)$, making it impractical for most large systems. However, specific sparse algorithms exist which discard the zero elements, drastically reducing the computational cost. Similarly, other factorizations which one might generally use to solve a dense system, such as QR, SVD, and Cholesky have analogous sparse algorithms which ignore all zero elements.

Once a factorization has been computed, solving the system is extremely cheap. This makes factorization particularly appealing in cases where it is necessary to solve numerous systems with the same coefficient matrix A, but for different right-hand side vectors b. This occurs in particular for linear time-dependent PDEs. However, since we are considering the time-independent RTE, that appeal is lost on us.

Another major limitation of factorizations is the large amount of memory they require. Fundamentally, factorizations require the storage of multiple factors, which need not necessarily preserve the sparsity pattern of the original matrix. This limitation is somewhat avoidable with out-of-core computations, whereby matrices are stored directly on the hard drive rather than in memory. Computations directly on disk, however, are anywhere from 6 to 10^5 times slower than computations in memory [7].

3.2 Software Packages

Many implementations of direct methods exist for particular circumstances. `LAPACK` [3], the well known free and open source `FORTRAN` linear algebra library, contains subroutines for banded, triangular, symmetric, tridiagonal, and general matrices. Of those, the banded solver is potentially applicable to the system we consider. A variety of more sophisticated free and open source packages for solving sparse systems directly exist, such as `UMFPACK` [6] and `MUMPS` [1]. Both of these algorithms in particular are *multi-frontal*, which is to say that they only keep small slices (fronts) of the matrix in memory at any given time, and perform computations on several fronts in parallel, drastically reducing solution time.

4 Stationary Iterative Methods

4.1 Fixed-Point Iteration

Iterative methods are another way in which to solve linear systems of equations. Iterative methods work to successively improve upon their approximate solution, stopping when the results are calculated to within a tolerance which can be set as desired. Iterative methods are a generally good option for solving a linear system $Ax = b$ particularly when A is large. Since these systems meet that criteria, this was a path that was desirable to explore to see how these results compared.

We follow Anderson [2, Section 1.1] in describing basic Stationary Iterative Methods operate as follows. Given $Ax = b$, we choose N and P such that

$$A = N - P, \tag{18}$$

where N is invertible.

Then,

$$\begin{aligned} Ax &= b \\ (N - P)x &= b \\ Nx &= Px + b \end{aligned}$$

Extending the idea of fixed point iteration to systems, we take the two instances of x in the above equation to be consecutive iterates, and obtain

$$x^{(i+1)} = N^{-1}Px^{(i)} + N^{-1}b \tag{19}$$

Letting $G = N^{-1}P$ and $C = N^{-1}b$, we have the general form

$$x^{(i+1)} = Gx^{(i)} + C \tag{20}$$

The choice of N and P in the above equations determine the particular Stationary Iterative Method. In fact, given that

the two are related by (18), the choice of N uniquely defines a method.

The most common methods are listed here, where D, L, and U represent the diagonal, strictly lower triangular, and strictly upper triangular pieces of A respectively, I is the identity matrix, ω and p are free parameters for which the optimal value is problem-dependent.

Method	N
Jacobi	D
JOR	$\frac{1}{\omega}D$
Gauss-Seidel	$D + L$
SOR	$\frac{1}{\omega}D + L$
Richardson	$-\frac{1}{p}I$

Figure 8: Basic Linear Stationary Iterative Methods [12]

4.2 Convergence and Preconditioning

It is a well-known result [2] that the iterative method defined by (20) converges to the exact solution x if and only if $\rho(G) < 1$, where $\rho(G)$ is the *spectral radius* of G, defined as the largest modulus of an eigenvalue of G. A sufficient but unnecessary condition for convergence of (20) is the diagonal dominance of A.

As we observed in section 2.5.1, A is in general not diagonally dominant for this problem. Further, we show that it's eigenvalues need not be bounded in the unit circle.

4.2.1 Gershgorin Disks

Some modification to precondition the system would be necessary in order to run either of these methods. Two feasible options were concluded upon. The first option would be to compute the SVD and then use U and V^T to precondition the matrix. However, the SVD is an expensive computation and can be used directly to solve the system. Since this was being done within the scope of the project, this option was eliminated. The other option was to use Jacobi iterations to identify and gradually reduce the off-diagonal terms. This serves to make the system increasingly diagonally dominant until it eventually becomes solvable through these Stationary Iterative Methods.

Code was developed and proven in reducing the off-diagonal terms to where both of the methods would converge. The negative was that the initial systems were fairly far from diagonal dominance, determining the number of iterations the algorithm would take to solve. As a result, this was actually far slower than a direct SVD computation. There might be some value if these computations were to be run over and over again having computed the preconditioner, but generally appears to make these solutions not competitive with other options.

Since this was proven to work, one of the smaller systems were utilized to see what kind of results would be obtained from this point using these methods. The systems were both run with a tolerance of `1e-3` and an initial guess of a zero vector.

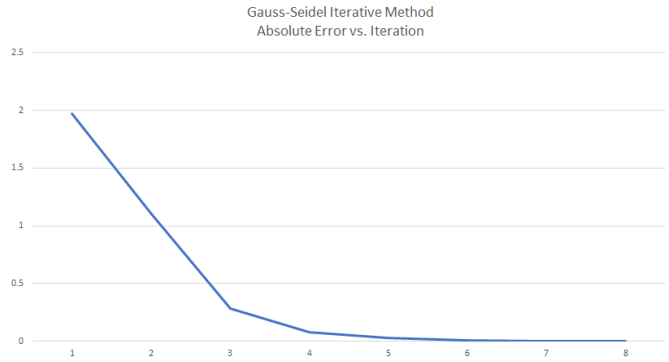

The Jacobi method ran in 47 iterations, taking a total computation time of 3.85 seconds.

In this case, the Gauss-Seidel method was faster and less expensive. It completed in 8 iterations and taking a total time of 0. 75 seconds. It is also worth noting that fewer Jacobi iterations were necessary in the preconditioning process to allow the Gauss-Seidel method to begin to converge, further making this method more effective for this particular system.

In conclusion, the results demonstrated that these methods could be effective and produce useful results in reasonable computation times. The major negative was the time and cost involved in preconditioning as a result of the systems not being naturally structured to be convergent through these methods. To get an idea of the cost, the iterative methods took on the order of seconds or less as indicated by the sample system above. The process to precondition took on the order of tens of minutes into hours even for smaller systems.

5 Nonstationary Iterative Methods

5.1 Krylov Subspace Methods

5.2 Convergence and Preconditioning

5.2.1 Eigenvalue Clustering

6 Numerical Results

7 Conclusions

References

[1] P. Amestoy, I. S. Duff, J.-Y. L'Excellent, and J. Koster. MUMPS: A General Purpose Distributed Memory

Sparse Solver. In *Proceedings of the 5th International Workshop on Applied Parallel Computing, New Paradigms for HPC in Industry and Academia*, PARA '00, pages 121–130, London, UK, UK, 2001. Springer-Verlag. ISBN 3-540-41729-X. URL http://dl.acm.org/citation.cfm?id=645782.666826.

[2] C. J. Anderson. *Analysis of Controlled Over-Relaxation*. PhD thesis, University of Akron, 2012. URL http://rave.ohiolink.edu/etdc/view?acc_num=akron1342456200.

[3] E. Anderson, Z. Bai, C. Bischof, S. Blackford, J. Demmel, J. Dongarra, J. Du Croz, A. Greenbaum, S. Hammarling, A. McKenney, and D. Sorensen. *LAPACK Users' Guide*. Society for Industrial and Applied Mathematics, Philadelphia, PA, third edition, 1999. ISBN 0-89871-447-8 (paperback).

[4] A. H. Baker, E. R. Jessup, and T. Manteuffel. A Technique for Accelerating the Convergence of Restarted GMRES. *SIAM Journal on Matrix Analysis and Applications*, 26(4):962–984, Jan. 2005. ISSN 0895-4798, 1095-7162. doi: 10.1137/S0895479803422014. URL http://epubs.siam.org/doi/10.1137/S0895479803422014.

[5] S. Chandrasekhar. *Radiative Transfer*. Dover, 1960. URL https://archive.org/details/RadiativeTransfer.

[6] T. A. Davis. Algorithm 832: UMFPACK V4. 3an unsymmetric-pattern multifrontal method. *ACM Transactions on Mathematical Software (TOMS)*, 30(2):196–199, 2004. URL http://dl.acm.org/citation.cfm?id=992206.

[7] A. Jacobs. The pathologies of big data. *Communications of the ACM*, 52(8):36–44, 2009. URL http://dl.acm.org/citation.cfm?id=1536632.

[8] E. Jones, T. Oliphant, P. Peterson, and others. *SciPy: Open source scientific tools for Python*. 2001. URL http://www.scipy.org.

[9] C. Mobley. Radiative Transfer in the Ocean. In *Encyclopedia of Ocean Sciences*, pages 2321–2330. Elsevier, 2001. ISBN 978-0-12-227430-5. URL http://linkinghub.elsevier.com/retrieve/pii/B012227430X004694.

[10] J. Nocedal and S. J. Wright. *Numerical optimization*. Springer series in operations research. Springer, New York, 1999. ISBN 978-0-387-98793-4.

[11] F. Prez and B. E. Granger. IPython: a system for interactive scientific computing. *Computing in Science & Engineering*, 9(3):21–29, May 2007. ISSN 1521-9615. doi: 10.1109/MCSE.2007.53. URL http://ipython.org.

[12] D. Young. *Iterative solution of large linear systems*. Computer science and applied mathematics. Academic Press, 1971. URL https://books.google.com/books?id=oALvAAAAMAAJ.